Journal of Lake and Reservoir Management 14(2-3):290-300, 1998

Development and Parameterization of a Kinetic Framework for Modeling Light- and Phosphorus-Limited Phytoplankton Growth in Cannonsville Reservoir[1]

Martin T. Auer
Department of Civil and Environmental Engineering
Michigan Technological University
Houghton, MI 49931-1295

B. Forrer
Ch2M Hill/STL
10 South Broadsay, Suite 450
St. Louis, MO 63102

ABSTRACT

Auer, M. T. 1998. Development and parameterization of a kinetic framework for modeling light-and phosphorus-limited phytoplankton growth in Cannonsville Reservoir. Lake and Reserv. Manage. 14(2-3):290-300.

A mechanistic framework for simulating phytoplankton growth kinetics in lakes and reservoirs is described. The framework is based on published physiological submodels describing light-and phosphorus-limitation of phytoplankton growth and the relationship between the rates of growth and respiration. The physiological submodels were tested and related kinetic coefficients defined through a program of field measurement and laboratory experimentation. Values for kinetic coefficients were determined using the natural phytoplankton assemblage of Cannonsville Reservoir, a part of the New York City drinking water supply system. The suite of submodels was shown to satisfactorily represent the phytoplankton response to variation in the light and nutrient regime of the reservoir. Efforts to test submodels and determine kinetic coefficients on a site-specific basis are believed to enhance the credibility and reliability of the model framework in its application for water quality management.

Key Words: algal growth, lakes, light limitation, modeling, phosphorus, phytoplankton kinetics, reservoirs, respiration.

Mathematical models are widely used to support the development of water quality management plans for lakes and reservoirs. Current management models focus on nutrient-food web dynamics and are significantly more complex than the empirical correlations and simple budget models widely applied in the past (Chapra and Auer 1998). The greater mechanistic resolution afforded by nutrient-food web models comes at a cost: algorithms for component submodels must be developed and values for kinetic coefficients defined. The supporting science must keep pace with developments in complexity in order to maintain a satisfactory level of model reliability. Our research group has promoted an 'integrated approach' to modeling (Auer and Canale 1986; Auer and Niehaus 1993; Canale et al. 1993; Canale et al. 1995; Doerr et al. 1996), where submodels are tested and model coefficients determined on a site-specific basis through companion programs of field monitoring and laboratory experimentation.

Here we present a kinetic framework for modeling light- and phosphorus-limited phytoplankton growth built from published physiological submodels. We describe the suite of field measurements and laboratory experiments used to verify these submodels and to determine values for associated kinetic coefficients for Cannonsville Reservoir (New York), a part of the New York City water supply. Our approach builds on previous efforts in Green Bay, Lake Michigan (Auer et al. 1986) and Onondaga Lake, New York (Storey et al. 1993) where natural phytoplankton assemblages were used to obtain site-specific information on nutrient and phytoplankton dynamics. The kinetic framework presented here was used by Doerr et al. (1998) in developing a comprehensive water quality model for the reservoir.

[1]Contribution No. 187 of the Upstate Freshwater Institute.

Theoretical Basis

Mechanistic phytoplankton growth models (cf. Chapra 1997) are based on mass balances on algal standing crop (e.g. carbon, chlorophyll, dry weight) and one or more growth-limiting nutrients (taken here to be phosphorus, P). Mass balance equations for the growth limiting nutrient may be written for both material in the water (dissolved or external P) and that stored within the alga (cellular or internal P).

$$\frac{dX}{dt} = [\mu - k_L] \cdot X \tag{1}$$

$$\frac{dP}{dt} = \text{sources} - \text{sinks} - \rho \cdot X \tag{2}$$

$$\frac{dQ}{dt} = \rho - \mu \cdot Q \tag{3}$$

where X is a measure of phytoplankton biomass ($\mu gChl \cdot L^{-1}$); μ is the specific growth rate coefficient (d^{-1}); k_L is a first-order coefficient which quantifies losses to grazing, respiration, and settling (d^{-1}); P is the external P concentration ($\mu gP \cdot L^{-1}$); ρ is the specific phosphorus uptake rate ($\mu gP \cdot \mu gChl^{-1} \cdot d^{-1}$); and Q is the internal P concentration, often termed the cell quota ($\mu gP \cdot \mu gChl^{-1}$).

A variety of physiological submodels (cf. Bowie et al. 1985; Chapra 1997) may be applied to describe the role of environmental factors in mediating nutrient and phytoplankton dynamics. For example, μ may be modified to accommodate the effects of light and nutrient availability:

$$\mu = \mu_{max,T} \cdot \phi_P \cdot \phi_I \tag{4}$$

where $\mu_{max,T}$ is the maximum specific growth rate coefficient (d^{-1}) at a particular temperature (for optimum light and excess nutrients) and where ϕ_P and ϕ_I are dimensionless attenuation factors (range, 0→1) for phosphorus and light limitation, respectively.

Two approaches have been most commonly (cf. Bierman and Dolan 1981; Bowie et al. 1985; Chapra 1997) used in defining the attenuation factor for phosphorus (ϕ_P): the Monod model (Monod 1950; see also Auer and Canale 1982a and Auer et al. 1986), based on external P concentration, and the Droop model (Droop 1974; see also Auer and Canale 1982a and Auer et al. 1986), based on internal P concentration. The Monod model relates the attenuation factor to the external (usually soluble reactive or orthophosphate) P pool:

$$\phi_P = \frac{P}{k_p + P} \tag{5}$$

where k_p is the half-saturation constant for growth as a function of the external P concentration ($\mu gP \cdot L^{-1}$). The magnitude of k_p reflects the affinity of the organism or assemblage for P, i.e., the ability to acquire the nutrient at low concentrations. In the Droop model, the attenuation coefficient is related to the internal P pool:

$$\phi_P = 1 - \frac{Q_0}{Q} \tag{6}$$

where Q_0 is the minimum cell quota, representing a starvation level of limiting nutrient where growth ceases. Contributions to the internal nutrient pool are made through phosphorus uptake as described by Michaelis-Menten (Michaelis-Menten 1913) kinetics:

$$\rho = \rho_{max} \cdot \frac{P}{k_m + P} \tag{7}$$

where ρ_{max} is the maximum P uptake rate ($\mu gP \cdot \mu gChl^{-1} \cdot d^{-1}$) and k_m is the half-saturation constant for P uptake ($\mu gP \cdot L^{-1}$).

Two models are also routinely (cf. Bowie et al. 1985; Thomann and Mueller 1987; Chapra 1997) applied for simulation of the light attenuation factor (ϕ_I). The first is a saturation function similar in form to the Monod model:

$$\phi_I = \frac{I}{k_I + I} \tag{8}$$

where I is light intensity (PAR, $\mu E \cdot m^{-2} \cdot s^{-1}$) and k_I is the half-saturation constant for growth as a function of light (PAR, $\mu E \cdot m^{-2} \cdot s^{-1}$). A second model, the Steele (1965) function, accommodates the observation that growth may be inhibited at high light intensities and defines an optimum light level for growth (I_{opt}, $\mu E \cdot m^{-2} \cdot s^{-1}$):

$$\phi_I = \frac{I}{I_{opt}} \cdot e^{-\frac{I}{I_{opt}}+1} \tag{9}$$

The loss term (k_L) identified in Equation 1 accommodates settling, grazing, and respiration – the latter being the only intrinsic feature related to net production. Laws and Chalup (1990) have proposed that algal respiration be described as a basal rate, increasing in proportion to the growth rate of the algae:

$$k_r = k_{basal} + \phi_R \cdot u \tag{10}$$

where k_r is the respiration rate coefficient (d^{-1}), k_{basal} is the maintenance or dark respiration rate coefficient (d^{-1}), and ϕ_R is a dimensionless multiplier relating the rates of respiration and growth.

The final model framework for simulating phytoplankton growth as a function of light intensity and levels of external and internal P is achieved by

substituting the submodels presented as Equations 4-10 to Equations 1-3.

Methods and Materials

Experimental Design

Two types of experiments were conducted, both using the natural phytoplankton assemblage of Cannonsville Reservoir. The first type was a series of 'light-dark bottle' (change in dissolved oxygen) incubations to determine values for the coefficients defining rates of photosynthesis and respiration. An aliquot of water was spiked with phosphorus to assure nutrient saturation and incubated over a range of light intensities yielding values for $\mu_{max,T}$ (Eq. 4), k_I (Eq. 8), I_{opt} (Eq. 9), and k_{basal} and ϕ_R (Eq. 10). Paired 'light-dark bottle' experiments, conducted on unspiked samples and accompanied by characterization of external and internal nutrient levels, were used to derive estimates of $\mu_{max,T}$ (Eq. 4), k_p (Eq. 5), and Q_0 (Eq. 6). The second type of experiment employed radioisotopes to measure rates of phosphorus uptake and establish values for the coefficients ρ_{max} and k_m (Eq. 7).

Experimental Protocol

Field Methods

A gradient in algal standing crop and phosphorus levels exists along the major longitudinal axis of Cannonsville Reservoir in response to discharges from the West Branch of the Delaware River, the system's major tributary (Effler and Bader 1998). Nutrient conditions also vary temporally with a switch from phosphorus to nitrogen limitation in mid- to late-summer. The ratio of nitrate-nitrogen (NO_3-N) to soluble reactive phosphorus (SRP) in water samples (Effler and Bader 1998) was used to identify the limiting nutrient. The guidelines of OECD (1982) were applied in establishing the boundary between N and P limitation with N:P ratios $\geq$15:1 corresponding to P-limitation. More than order of magnitude differences in algal standing crop and internal and external phosphorus were observed over the study period. This degree of spatial and temporal variability is ideal for the study of nutrient effects on phytoplankton growth.

Surface water grab samples were collected from six stations on the reservoir (cf. Effler and Bader 1998) between April and October 1995; an additional sample was collected at Station 4 for respiration experiments on 14 September 1997. Samples were split into two aliquots, and one aliquot was spiked with phosphorus (as KH_2PO_4, to a concentration 150 $\mu gP \cdot L^{-1}$ above ambient). This level of P addition insured phosphorus saturation ($Q \geq 2\ \mu gP \cdot \mu gChl^{-1}$) for chlorophyll levels in excess of 75 $\mu gChl \cdot L^{-1}$, well within the bounds of algal standing crop for these experiments. Samples were then shipped on ice to laboratories at Michigan Technological University, arriving the day following collection.

Laboratory Methods

Upon receipt at the laboratory, samples were placed in an incubator at 20 °C and aerated under saturating light conditions (600 $\mu E \cdot m^{-2} \cdot s^{-1}$) for 12 hours to acclimate to experimental conditions. Samples were analyzed for chlorophyll (Parsons et al. 1984) and soluble reactive, total dissolved (TDP), dissolved organic (DOP = TDP-SRP) and particulate (PP) phosphorus (APHA 1992) prior to each experiment.

Spiked and unspiked samples were incubated at 20 °C over a range of light intensities (0 to 1200 $\mu E \cdot m^{-2} \cdot s^{-1}$) and photosynthesis and respiration were measured as oxygen production and consumption, respectively, with an Orion Research electrode (Model 97-08). Rates of oxygen production and consumption were converted to specific rates of growth and respiration as described below:

$$\mu, k_r = \frac{R_{02} \cdot 10^3}{X \cdot r_{C:Chl} \cdot PQ} \qquad (11)$$

where R_{O2} is the rate of oxygen production or consumption ($mgO_2 \cdot L^{-1} \cdot d^{-1}$), $r_{C:Chl}$ is the carbon to chlorophyll ratio (80 $\mu gC \cdot \mu gChl^{-1}$), and PQ is the photosynthetic quotient (32 $\mu gO_2 \cdot 12\ \mu gC^{-1}$) and 10^3 converts mg to μg. Light-enhanced and basal respiration (measured on spiked samples) were defined as the rates of oxygen consumption immediately and 12 hours after the lights were turned off. Growth rate data for spiked samples were fit to the functions presented as Eq. 8 and 9 to test the utility of these models for the light-growth response and to provide estimates of $\mu_{max,T}$, k_I, and I_{opt}. Growth and respiration rate data for spiked samples were fit to the function presented as Eq. 10 to test the model proposed by Laws and Chalup (1990) and to derive values for k_{basal} and ϕ_R. Growth rate data for unspiked samples were fit to the functions presented as Eq. 5 and 6 to evaluate the role of phosphorus as the nutrient limiting algal growth and to provide estimates of k_p and Q_0.

Phosphorus uptake rates were measured by adding orthophosphorus at levels of 0, 1, 2, 4, 12, 20, and 40 $\mu gP \cdot L^{-1}$ above ambient (0.6 to 4.4 $\mu gP \cdot L^{-1}$) to otherwise unspiked samples. These enrichments then received phosphoric acid labeled with ^{32}P (New England Nuclear) at a specific activity of (17 $\mu Ci \cdot mL^{-1}$) and were

incubated at a saturating light intensity (600 $\mu E \cdot m^{-2} \cdot s^{-1}$) for 40 minutes (because the uptake-substrate relationship becomes nonlinear with time). Subsamples were collected at 5-minute intervals and filtered through 3.0- and 0.45-µm membranes to separate algal and heterotrophic bacterial uptake (cf. Currie and Kalff 1984). Algal uptake dominated in all experiments and only those results (3.0-µm filter) are presented here. The filters were transferred to scintillation vials, 10 ml of liquid scintillation cocktail was added (ScintiVerse BD; Fisher) and radioactivity was measured using a Beckman LS1801 liquid scintillation counter (counting efficiency = 81%). Volumetric phosphorus uptake rates ($\mu gP \cdot L^{-1} \cdot d^{-1}$) were calculated for each enrichment level as the initial slope of a plot of the mass of P incorporated into the particulate phase versus time and converted to chlorophyll-specific rates by dividing by the chlorophyll concentration. Rates of chlorophyll-specific phosphorus uptake at each enrichment level were then fit to the function presented as Eq. 7 to provide estimates of ρ_{max} and k_m.

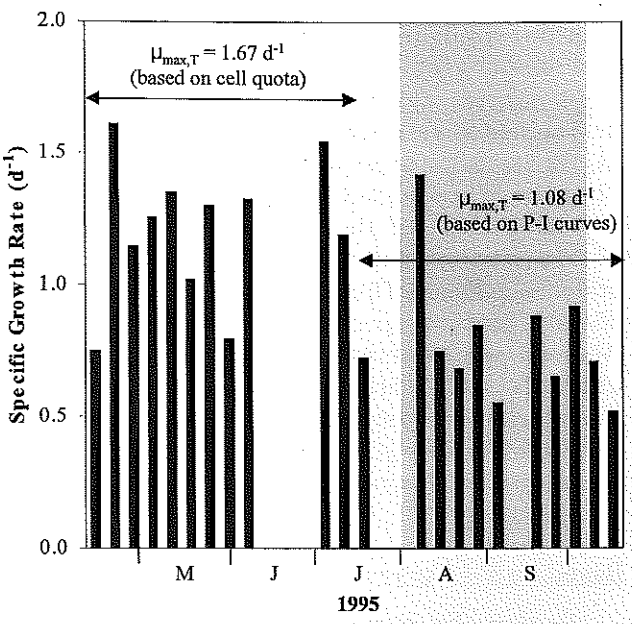

Figure 1.–Specific growth rate, mean for all stations, under ambient nutrient conditions. Shading indicates period of nitrogen limitation as defined in text.

Results and Discussion

Specific Growth Rate (µ)

Measurements of photosynthesis made at saturating light intensities (600 $\mu E \cdot m^{-2} \cdot s^{-1}$) on unspiked samples were used to determine the specific growth rate of the natural phytoplankton assemblage under ambient nutrient conditions (Fig. 1). Growth rates were reasonably constant (see results below) within periods characterized by phosphorus (11 April – 25 July and 10 October – 13 November) and nitrogen (1 August – 3 October) limitation, respectively (Fig. 2). The transition to N-limitation was characterized by a shift in the phytoplankton from a diatom-cryptomonad assemblage to one dominated by cyanobacteria and, later, cryptomonads. The return to P-limitation in the fall was accompanied by another shift, here to an assemblage dominated by diatoms (Siegfried, unpub. data). During P-limitation, the specific growth rate (mean for all stations) ranged from 0.52 to 1.61 d^{-1} with a reservoir-wide mean of 1.11 ±0.33 d^{-1}. Under N-limitation, the specific growth rate was somewhat lower, ranging from 0.56 to 1.42 d^{-1} with a mean of 0.84 ±0.27 d^{-1}. The variation in the specific growth rate within these periods is of a magnitude expected for observed fluctuations in the phosphorus status of the water column (SRP = 2.8 ±1.7 $\mu gP \cdot L^{-1}$; ϕ_p = 0.7-0.9, based on the Monod model and k_p as determined below. The difference in average specific growth rates between the P- and N-limited periods is also well within the bounds for growth rate variation among algal groups (cf. Bowie et al. 1985).

Maximum Specific Growth Rate ($\mu_{max,T}$)

Based on Cell Quota

An estimate for the maximum specific growth rate was derived from measurements of photosynthesis made

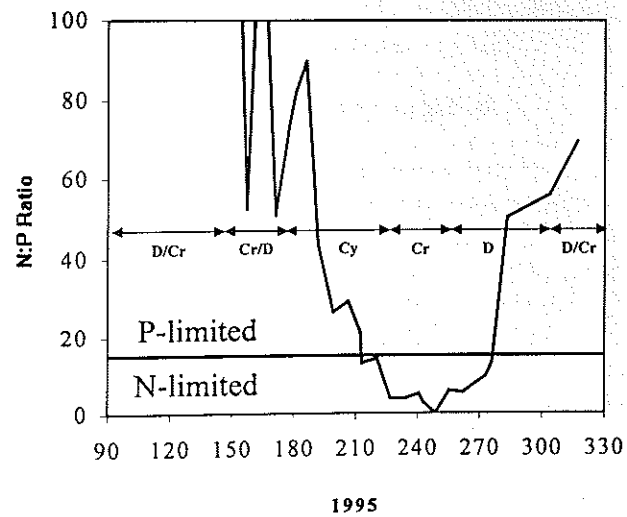

Figure 2.–N:P ratio (as NO_3-N:SRP) used in defining conditions of nitrogen- and phosphorus limitation. Solid line indicates boundary, N:P = 15:1. Lettered notation identifies dominant phytoplankton groups: D = diatoms, Cr = cryptomonads, Cy = cyanobacteria (Siegfried, unpubl. data).

at a saturating light intensity on unspiked samples from each sampling station, i.e., representing a range in ambient nutrient conditions. The value for $\mu_{max,T}$ was determined as the slope of a plot (Fig. 3a) of Q versus μQ (linearization of Eq. 6; cf. Auer and Canale 1982a). The analysis was limited to the April to July period of P-limitation because the relationship between phosphorus cell quota and growth rate (Eq. 6) is not valid under N-limitation. The value for $\mu_{max,T}$ so derived is 1.67 ±0.6 d^{-1}. Ambient specific growth rates during this P-limited period averaged 66% of μ_{max}, i.e., $\phi_p = 0.66$. This aver-age ambient rate is less than would be expected based on the Droop model which predicts a $\phi_p = 0.83$ for a Q_0 of 0.29 μgP·μgChl^{-1} (as determined below) and the measured reservoir-wide period-average Q of 1.7 μgP·μgChl^{-1}.

Based on P-I Curves

During the period of N-limitation, N-fixing cyanobacteria dominated the plankton assemblage and $\mu_{max,T}$ was estimated from photosynthesis measurements made on P-spiked samples, i.e., neither N nor P were limiting. Incubation of samples over a range of light intensities yields photosynthesis-irradiance (P-I) curves (Fig. 3b) with $\mu_{max,T}$ determined as the asymptote for the light-saturation model (Eq. 8) or the maximum value for the light-inhibition (Eq. 9) model. Experiments were conducted on a weekly basis over the period 1 August to 17 October 1995. The mean value for $\mu_{max,T}$ over this period was 1.08 ±0.6 d^{-1}, with a range of 0.28 to 2.48 d^{-1} (Table 1). Ambient specific growth rates averaged 78% of $\mu_{max,T}$ over this interval (Fig. 1), nearer the maximum than for P-limited conditions and consistent with the higher reservoir-wide cell quota values observed at this time (averaging 3.0 μgP·μgChl^{-1}). Differences in the μ_{max} estimates for N- and P-limited periods corresponded to species shifts in the phytoplankton.

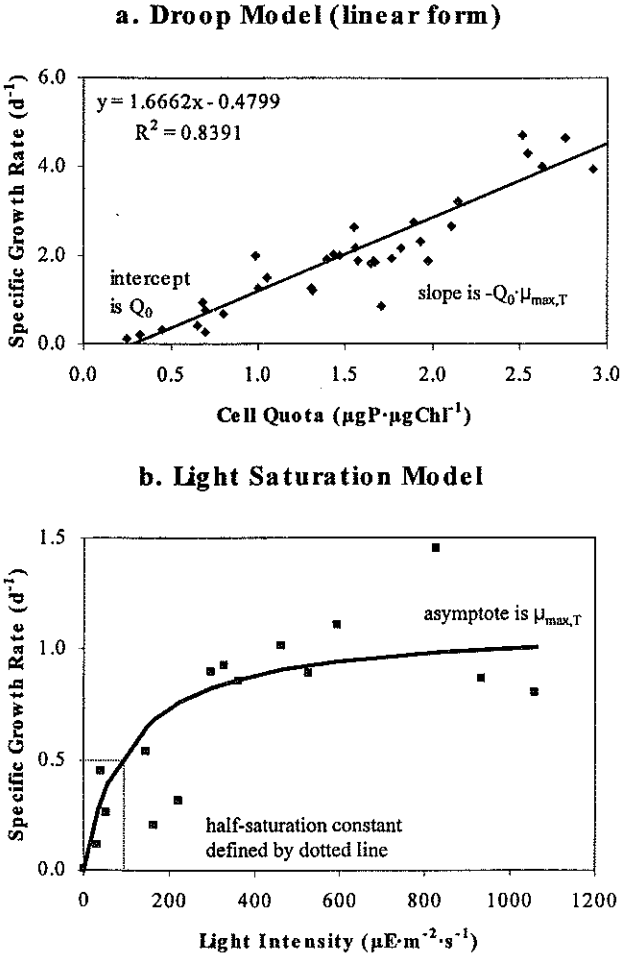

Figure 3.–Determination of the maximum specific growth rate ($\mu_{max,T}$) through application of (a) the Droop model for nutrient limitation and (b) the saturation model for light limitation.

Growth and Nutrients (k_p, Q_0)

Paired measurements of growth rate (unspiked samples) and phosphorus chemistry were used to determine values for the kinetic coefficients embodied in the physiological submodels which characterize ϕ_p. A plot of growth rate as a function of SRP (Fig. 4a with $\mu_{max,T} = 1.67$ d^{-1}) fit to the Monod model (Eq. 5) yields the value of the half-saturation constant for growth ($k_p = 0.5$ μgP·L^{-1}). The value for k_p lies close to the limit of analytical detection for SRP indicating that the phytoplankton assemblage can acquire P at very low levels. The coincidence of a low k_p and low ambient external P levels imparts considerable uncertainty to the application of the Monod model as all terms in Eq. 5 are at or near the analytical detection limit. An additional concern in application of the Monod model (cf. Chapra 1997) lies with the knowledge that low ambient external P levels do not necessarily reflect conditions of growth limitation because internal P levels may remain sufficient for extended periods following P depletion in the water column (Auer and Canale 1982b). Application of the Droop model evolved in response to these problems.

Growth rate data were plotted as a function of DOP concentration to test the Monod model for this potential phosphorus source. The DOP pool is used by algae once SRP has been depleted below some critical level (e.g., 1 to 2 μgP(L^{-1}; Connors et al. 1996) activating the enzyme systems which mediate DOP hydrolysis. Although SRP levels were often near or below this threshold (Fig. 5, left panels) and a slow, but systematic depletion of DOP was evident (Fig. 5, left panels), there was no apparent relationship between DOP concentration and growth rate. DOP utilization

Table 1.–Kinetic coefficients derived from P-I curves.

Date	Response	$\mu_{max,T}$ (d^{-1})	k_I ($\mu E \cdot m^{-2} \cdot s^{-1}$)	I_{opt} ($\mu E \cdot m^{-2} \cdot s^{-1}$)	Dominant Group
8/1	Saturation - low k_I	1.08	20	–	Cyanobacteria
8/8	Saturation - low k_I	0.84	20	–	Cyanobacteria
8/15	Saturation - low k_I	0.94	75	–	Cryptomonads
8/22	Saturation - low k_I	1.08	75	–	Dinoflagellates
8/29	Saturation - low k_I	0.56	75	–	Cryptomonads
9/5	Saturation - low k_I	2.48	40	–	-nd-
9/12	Saturation - high k_I	1.78	140	–	Cryptomonads
9/19	Saturation - low k_I	0.42	20		Diatoms
9/26	Inhibition	0.28		250	Dinoflagellates
10/3	Inhibition	0.75	–	300	Diatoms
10/10	Saturation - high k_I	1.64	300		Diatoms
10/17	Saturation - high k_I	1.08	150		Diatoms

and growth rate may appear to be uncoupled because DOP is converted to SRP prior to uptake. In this case, growth rate would be related directly to SRP levels (and indirectly to the rate of DOP hydrolysis) rather than directly to DOP concentrations.

The Droop model (Eq. 6) provides an alternative to the Monod model, describing the relationship between growth rate and cell quota (Fig. 4b). The linearized form of Eq. 6 has an intercept of $-Q_0 \cdot \mu_{max}$ which can be used to determine the value for the minimum cell quota (Fig. 3a). A linear regression of these data yields values for $\mu_{max,T}$ and Q_0 of 1.67±0.6 d^{-1} and 0.29±0.27 $\mu gP \cdot \mu gChl^{-1}$, respectively. Phosphorus-limited conditions, as defined by the Droop model, occur below the inflection point in the Droop curve ($Q = 1 \rightarrow Q_0$; Fig. 4b; cf. Auer et al. 1986). Values for the cell quota approached the limiting region for brief periods in spring and in mid-summer (Fig. 5, right panels), but generally remained at levels associated with phosphorus sufficiency ($Q > 1$).

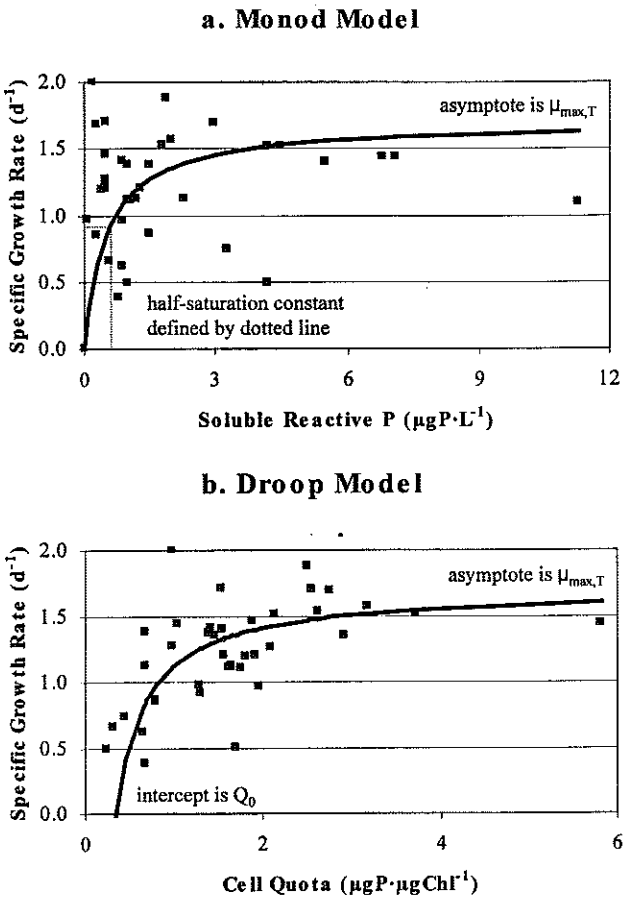

Figure 4.–Application of growth rates measured under ambient nutrient conditions in determining kinetic coefficients associated with (a) the Monod model ($\mu_{max,T}$ and k_p) and (b) the Droop model ($\mu_{max,T}$ and Q_0).

Nutrient Uptake (ρ_{max}, k_m)

Application of the Droop model for phosphorus-limited phytoplankton growth requires simulation of levels of external P (Eq. 2). Algal nutrient uptake, a process well described by Michaelis-Menten kinetics (Eq. 7), is a key term in the external P mass balance. Radioisotope measurements of phosphorus uptake (Fig. 6) were made on the natural phytoplankton assemblage using samples collected on five dates over the period 15 August – 12 September 1995. Uptake rates were plotted as a function of the external P (SRP) concentration (as illustrated in Fig. 6), yielding estimates for the maximum specific rate of phosphorus uptake (ρ_{max}, mean for all dates = 4.64 ±4.03 $\mu gP \cdot \mu gChl^{-1} \cdot d^{-1}$, range = 1.3 to 11.4) and the half-saturation constant for phosphorus uptake (k_m = 7.1 ±4.1 $\mu gP \cdot L^{-1}$, range = 4 to

14). Auer and Canale (1982b) demonstrated that variability in the magnitude of ρ_{max} and k_m could be associated with changes in the internal phosphorus pool. However, no systematic variation in cell quota was observed over the period when phosphorus uptake studies were conducted and Q levels in the reservoir remained within the saturated region (>2 μgP·μgChl^{-1}; Fig. 4b).

Growth and Light (I_{opt}, k_I)

Kinetic coefficients relating growth and light intensity were determined by fitting measurements of growth rate made on P-spiked samples over a range of light intensities to the light-saturation and light-inhibition functions introduced previously as Eqs. 8

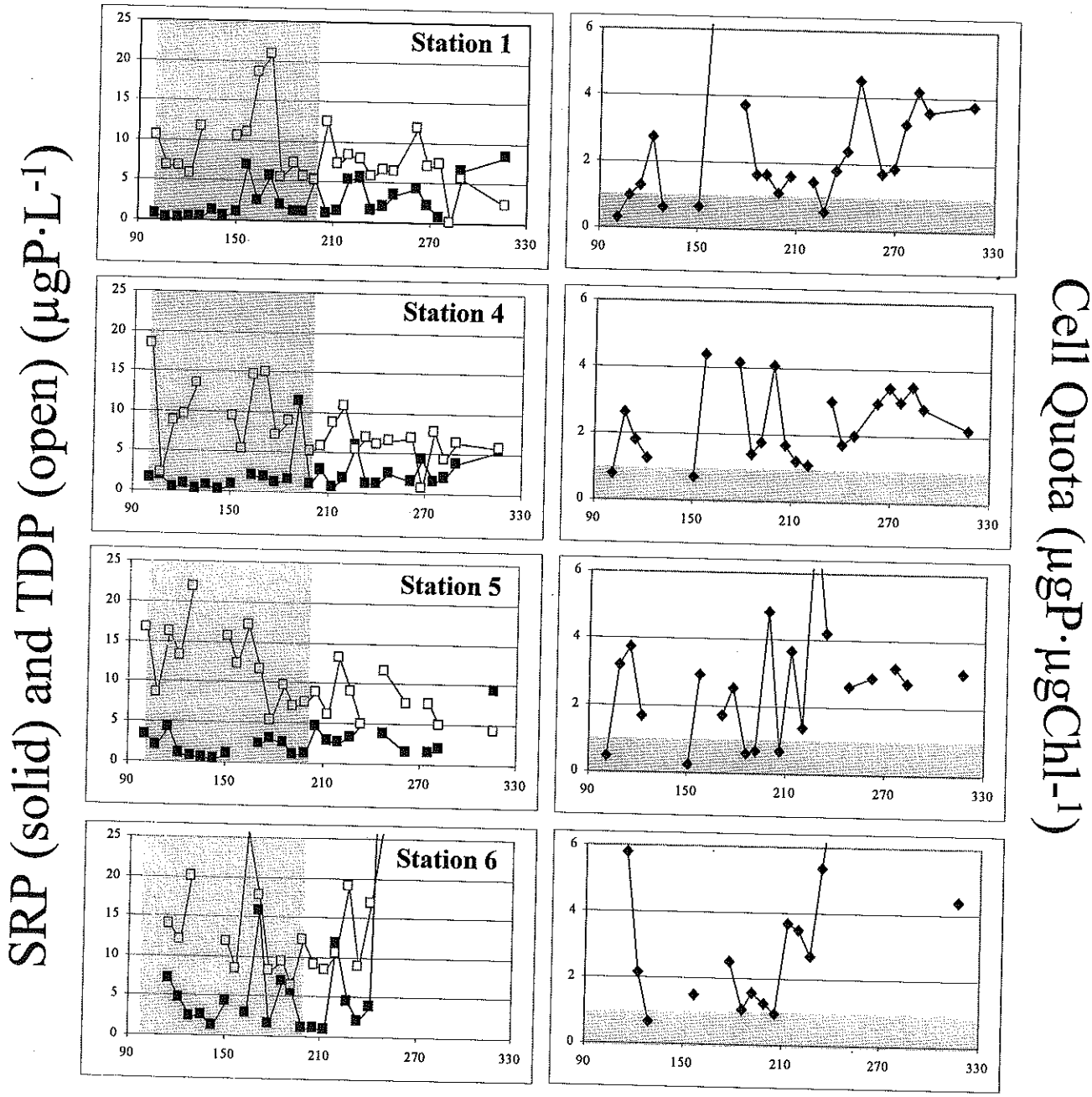

Figure 5.–Total dissolved and soluble reactive phosphorus (left panels) and cell quota (right panels) in Cannonsville Reservoir. Shaded area in left panels identifies period of P-limitation based on N:P ratio used for determination of growth rate. Shaded area in right panels identifies levels of cell quota indicative of P-limitation.

and 9. P-I curves were developed on 12 dates and exhibited 1 of 3 characteristic responses (Fig. 7): saturation/low k_I, saturation/high k_I, and inhibition. A saturation response with a low k_I was typical of the first eight experiments, inhibition for the next two, and a saturation response with a high k_I for the last two. Values for $\mu_{max,T}$ determined from these P-I curves were reported above. The mean values for k_I were 53 ± 37 $\mu E \cdot m^{-2} \cdot s^{-1}$ for the eight saturation response/low k_I experiments and 225 $\mu E \cdot m^{-2} \cdot s^{-1}$ for the two saturation response/high k_I experiments (Table 1). The average value for I_{opt} for the two experiments where inhibition was observed was 275 $\mu E \cdot m^{-2} \cdot s^{-1}$. The phytoplankton assemblage (Table 1) was largely dominated by cryptomonads and cyanobacteria during the period of saturation response/low k_I results and by diatoms and dinoflagellates during inhibition and saturation response/high k_I results (Siegfried, unpubl. data).

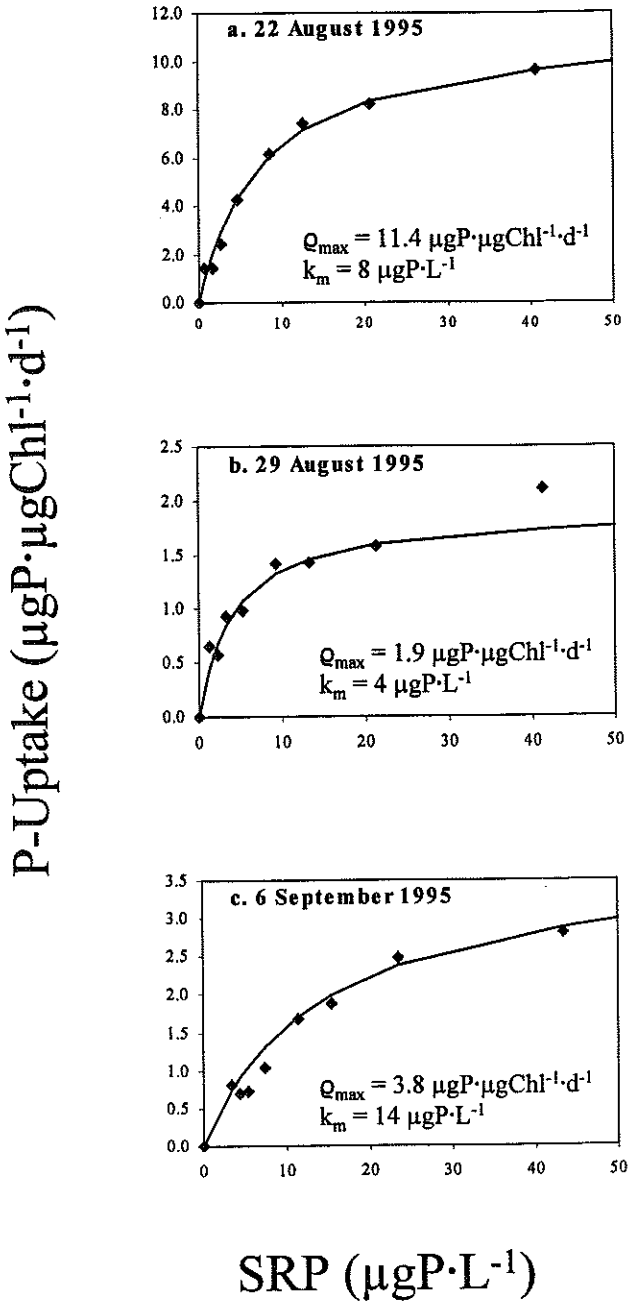

Figure 6.–Application of the Michaelis-Menten model in determining coefficients for phosphorus intake.

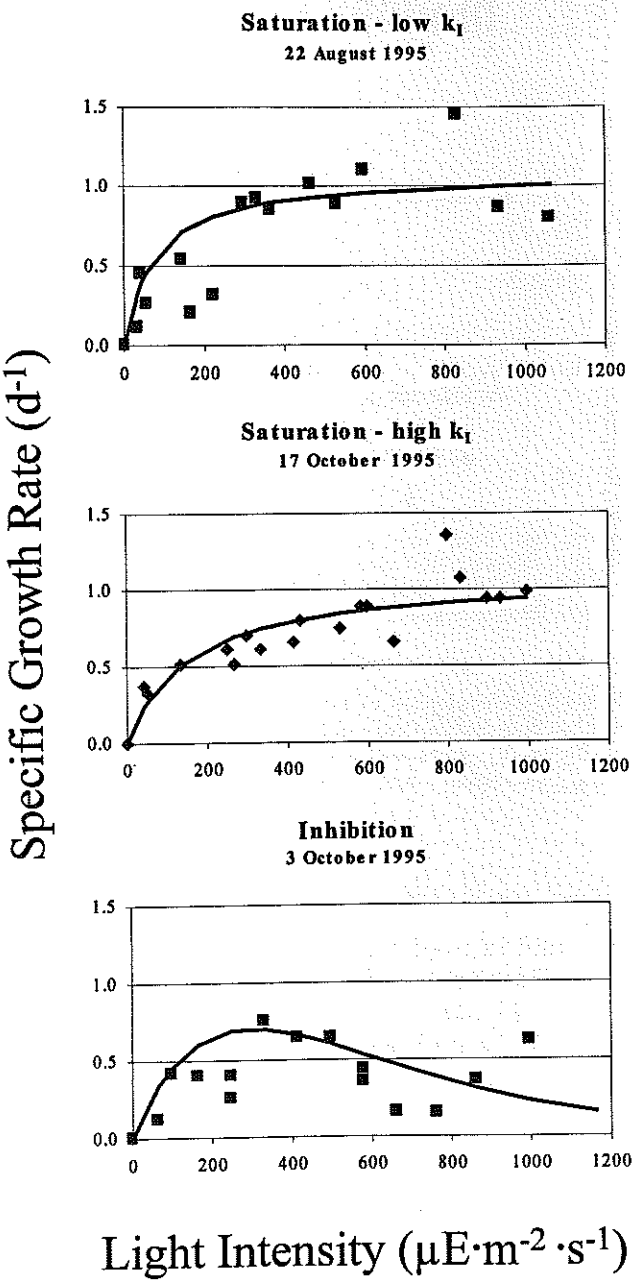

Figure 7.–Characteristic responses observed in the development of P-I curves.

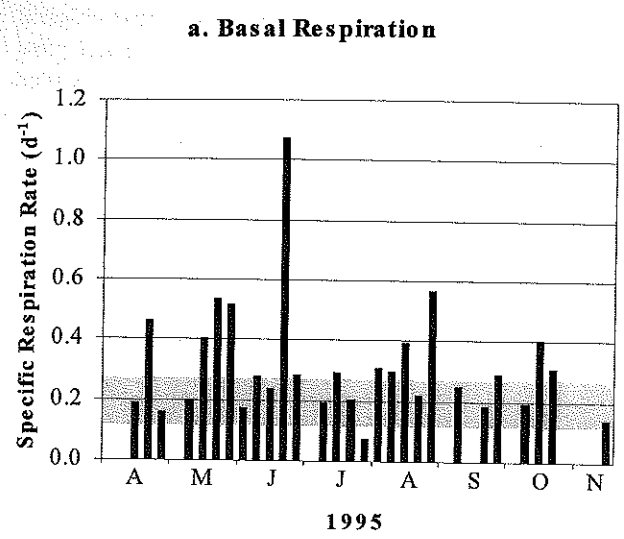

Figure 8.–Determination of (a) rates of basal respiration under ambient nutrient conditions and (b) values for the respiration rate coefficients k_{basal} and ϕ. Shaded area in the top panel illustrates fit of the k_{basal} coefficient to ambient measurements.

Respiration (k_{basal}, f_R)

Basal rates of community (algae plus bacteria) respiration were measured over the April to November interval of 1995 during 'light bottle-dark bottle' experiments. A regression of the volumetric rate of community respiration as a function of chlorophyll concentration yielded the specific rate of algal respiration as the slope and the volumetric rate of bacterial respiration as the intercept. The average rate of basal algal respiration over the study period was 0.3 ±0.2 d^{-1}, ranging from 0.08 to 1.1 d^{-1} (Fig. 8a).

The physiological submodel employed here for respiration (Eq. 10; Laws and Chalup 1990) represents the process as a basal rate, increasing linearly in proportion to the algal growth rate. Paired measurements of the growth and 'light-enhanced' respiration rate were then plotted (Fig. 8b), yielding the proportionality constant for respiration as the slope (ϕ_R = 0.23 ±0.16) and the basal respiration rate (k_{basal} = 0.20 ±0.08) as the intercept. The value for k_{basal} determined in this fashion compares well with that derived through regression (presented above) and provides a reasonable representation of ambient respiration rates (Fig. 8a).

Summary

A mechanistic framework for modeling the kinetics of light- and phosphorus-limited phytoplankton growth in lakes and reservoirs has been presented. The physiological submodels which constitute that framework, all derived from the literature, performed well in describing the relationship between rates of growth and respiration and ambient environmental conditions. Values for the kinetic coefficients embodied in that framework (summarized in Table 2) were determined through a program of field monitoring and laboratory experimentation. The magnitude of the coefficients and their degree of variation were shown to be consistent with the behavior of the phytoplankton assemblage (e.g., shifts in species composition) and the phosphorus status (e.g., degree and type of nutrient limitation) of the reservoir.

The selection of physiological submodels for inclusion in a kinetic framework should be guided by the degree of model resolution required. The cell quota approach for determination of $\mu_{max,T}$ provides a single estimate which integrates temporal and spatial variability in nutrient status and assemblage physiology appropriate for calculations over a seasonal time frame. Estimation of $\mu_{max,T}$ from P-I curves can provide coefficient values over much shorter intervals, useful in tracking changes in kinetics associated with shifts in species composition. The former approach utilizes unperturbed samples (no nutrient spiking) and thus may best represent the true nutrient physiology of the assemblage. Of the submodels tested for simulating P-limitation, the Droop formulation is to be preferred over the Monod approach where ambient P levels are near the limit of analytical detection. The Droop model does, however, require addition of cell quota as a state variable and simulation of uptake. The effects of light on respiration, at least under saturating intensities, are significant and this phenomenon should be included in the kinetic framework. The results presented here suggest that the capability to vary values for kinetic coefficients to accommodate shifts in species

Table 2.–Kinetic Coefficients

Coefficient	Notation	Units	Value
Maximum specific growth rate	$\mu_{max,T}$	d^{-1}	1.67 ±0.6 1.08 ±0.6
Half-saturation constant for growth as a function of external nutrient concentration	k_p	$\mu gP \cdot L^{-1}$	0.5
Minimum cell quota	Q_o	$\mu gP \cdot \mu gChl^{-1}$	0.29 ±0.27
Maximum specific uptake rate	ρ_{max}	$\mu gP \cdot \mu gChl^{-1} \cdot d^{-1}$	4.64 ±4.03
Half-saturation constant for uptake as a function of external nutrient concentration	k_m	$\mu gP \cdot L^{-1}$	7.1 ±4.1
Half-saturation constant for growth as a function of light intensity	k_I	$\mu E \cdot m^{-2} \cdot s^{-1}$	53 ±37
Optimal (saturating) light intensity	I_{opt}	$\mu E \cdot m^{-2} \cdot s^{-1}$	275
Basal respiration rate	k_{basal}	d^{-1}	0.20 ±0.08
Multiplier relating respiration and growth rate	ϕ_R	dimensionless	0.23 ±0.16

composition might be a valuable feature of the model (cf. DiToro and Connolly 1980; Bierman and Dolan 1981).

This research has demonstrated that published physiological submodels have utility in describing phytoplankton growth dynamics for Cannonsville Reservoir. The determination of kinetic coefficients on a site-specific basis is expected to enhance the reliability and credibility of the resulting model. Future demonstrations of the successful application of this framework to other lakes and reservoirs, especially those of differing trophic status, would offer further validation for the use of such models for management purposes. It is recommended that these results be applied in model sensitivity analyses to identify those kinetic coefficients meriting site-specific determination.

ACKNOWLEDGMENTS: The author wishes to thank Tracy Cavadeas for her assistance in carrying out photosynthesis and respiration experiments and Carol Brooks and Bruce Wagner for providing chlorophyll and phosphorus data. The contribution of Margaret Sottile in performing phosphorus uptake experiments is greatly appreciated. The critical comments of R. Thomas James and an anonymous reviewer are sincerely acknowledged. This study was supported by New York City Department of Environmental Protection.

References

American Public Health Association, American Water Works Association and Water Pollution Control Federation (APHA). 1992. Standard Methods for the Examination of Water and Wastewater, 18th Edition. American Public Health Association, Washington, DC.

Auer, M. T. and R. P. Canale. 1982a. Ecological studies and mathematics modeling of *Cladophora* in Lake Huron: 3. Dependence of growth rates on internal phosphorus pool size. J. Great Lakes Res. 8(1):93-99.

Auer, M. T. and R. P. Canale. 1982b. Ecological studies and mathematical modeling of *Cladophora* in Lake Huron: 2. Phosphorus uptake kinetics. J. Great Lakes Res. 8(1):84-92.

Auer, M. T. and R. P. Canale. 1986. Mathematical modeling of primary production in Green Bay (Lake Michigan, USA): A phosphorus and light-limited system. Hydrobiol. Bull. 20(2):195-211.

Auer, M. T. and S. L. Niehaus. 1993. Modeling fecal coliform bacteria: I. Field and laboratory determination of loss kinetics. Wat. Res. 27(4):693-701.

Auer, M. T., M. S. Kieser, and R. P. Canale. 1986. Identification of critical nutrient levels through field verification of models for phosphorus and phytoplankton growth. Can. J. Fish. Aquat. Sci., 43(2):379-388.

Bierman, V. J. Jr. and D. M. Dolan. 1981. Modeling of phytoplankton-nutrient dynamics in Saginaw Bay, Lake Huron. J. Great Lakes Res. 7(4):409-439.

Bowie, G. L., W. B. Mills, D. B. Porcella, C. L. Campbell, J. R. Pagenkopf, G. L. Rupp, K. M. Johnson, P. W. H. Chan, S. A. Gherini and C. Chamberlain. 1985. Rates, constants, and kinetic formulations in surface water quality modeling, 2nd Edition. EPA/600/3-85/040. U.S. Environmental Protection Agency, Athens, GA, 455 p.

Canale, R. P., M. T. Auer, E. M. Owens, T. M. Heidtke and S. W. Effler. 1993. Modeling fecal coliform bacteria: II. Model development and application. Wat. Res., 27(4):703-714.

Canale, R. P., E. M. Owens, M. T. Auer and S. W. Effler. 1995. Validation of water quality model for Seneca River, NY. J. Wat. Resour. Plan. Manage. 121(3):241-250.

Chapra, S. C. 1997. Surface Water-Quality Modeling, McGraw-Hill, New York, NY. 844 p.

Chapra, S. C. and M. T. Auer. 1998. Management models to evaluate phosphorus loads in lakes. *In:* K.R. Reddy (ed.). Phosphorus Biogeochemistry in Florida Ecosystems. In Press.

Connors, S. D., M. T. Auer and S. W. Effler. 1996. Phosphorus pools, alkaline phosphatase activity, and phosphorus limitation in hypereutrophic Onondaga Lake, N.Y. Lake and Reserv. Manage., 12(1):47-57.

Currie, D. J. and J. Kalff. 1984. The relative importance of bacterioplankton and phytoplankton in phosphorus uptake in fresh water. Limnol. Oceanogr. 29:311-321.

DiToro, D. M. and J. P. Connolly. 1980. Mathematical models of water quality in large lakes. Part 2. Lake Erie. EPA-600/3-80-065. U.S. Environmental Protection Agency, Duluth, MN. 231 p.

Doerr, S. M., R. P. Canale and S. W. Effler. 1996. Development and testing of a total phosphorus model for Onondaga Lake. Lake and Reserv. Manage. 12(1):141-150.

Doerr, S. M., E. M. Owens, R. K. Gelda, M. T. Auer and S. W. Effler. 1998. Development and testing of a nutrient-phytoplankton model for Cannonsville Reservoir. Lake and Reserv. Manage. 14(2-3):301-321.

Droop, M. R. 1974. The nutrient status of algal cells in continuous culture. J. Mar. Biol. Ass. U.K. 54:825-855.

Effler, S. W. and A. P. Bader. 1998. A limnological analysis of Cannonsville Reservoir, NY. Lake and Reserv. Manage. 14(2-3):125-139.

Laws, E. A. and M. S. Chalup. 1990. A microalgal growth model. Limnol. Oceanogr. 35:597-608.

Michaelis, L. and M. L. Menten. 1913. Die Kinetik der Invertinwirkung. Biochem. Z. 49:333-369.

Monod, J. 1950. La technique de culture continue theorie et application. Ann. Inst. Pasteur. 79:390-410.

OECD. 1982. Eutrophication of waters: Monitoring, assessment and control. Organisation for Economic Cooperation and Development. Paris, 154 p.

Parsons, T. R., Y. Maita and C. Lalli. 1984. A Manual of Chemical and Biological Methods for Seawater Analysis. Pergamon Press, New York. 173 p.

Steele, J. H. 1965. Notes on some theoretical problems in production ecology. P. 383-398. *In:* C.R. Goldman (ed.). Primary Production in Aquatic Environments, Univ. of California Press, Berkeley, CA.

Storey, M. L., M. T. Auer, A. K. Barth and J. M. Graham. 1993. Site-specific determination of kinetic coefficients for modeling algal growth. Ecol. Model. 66:181-196.

Thomann, R. V. and J.A. Mueller. 1987. Principles of Surface Water Quality and Control. Harper and Row, New York, NY. 644 p.